ChemComm

COMMUNICATION

View Article Online
View Journal | View Issue

Cite this: *Chem. Commun.*, 2026, **62**, 960

Received 25th October 2025,
Accepted 1st December 2025

DOI: 10.1039/d5cc06076a

rsc.li/chemcomm

Chromium-catalyzed reductive alkylation of *N*-heteroarenes using alkyl formates as transfer hydroalkylation reagents

Anit Pal, Asish Borah and Animesh Das *

Alkyl formates are employed as transfer hydroalkylation reagents in the reductive alkylation of *N*-heteroarenes to saturated azacycles. This is achieved using a well-defined chromium catalyst and LiI as a promoter *via* the cleavage of the C–O σ-bond of the formate, generating a hydride nucleophile and an alkyl electrophile. The reaction produces volatile CO_2 as the only byproduct, making the method atom-efficient and environmentally friendly.

The direct hydroalkylation reaction has found widespread applications in organic synthesis as it offers both reduction (hydro) and functionalization (alkylation) of unsaturated bonds such as alkenes or imines in an atom-economical manner.[1] In general, the reaction proceeds *via* a radical (1 electron mechanism) or non-radical (2 electron mechanism) pathway in the catalytic process.[2] Of these, the two-electron mechanism involving metal hydride as the active species represents the most efficient synthetic approach.

Owing to the ready accessibility of hydrocarbon substrates, this reaction has attracted significant attention. However, as this strategy requires the activation of inherently strong C–H alkyl bonds, its substrate scope is limited (*e.g.* acidic hydrogen-containing substrates).[3] As an alternative, transfer hydroalkylation has been well-studied[4,5] by Oshima (Rh-catalyzed hydroallylation),[4a] Tang (Lewis acid-promoted hydroalkylation of imines with Hantzsch esters),[4b] Akiyama (photocatalyzed hydroalkylation of activated alkenes with benzothiazole),[4c] Li (Ru or Pd-catalyzed alkylation of imines with hydrazones),[4d] Shibasaki (Cu-catalyzed hydroalkylation of aldimine using cyanocarboxylic acids),[4e] and Cantat (Ru-catalyzed reductive *N*-alkylation of imines with alkyl formate).[4f] However, most of these studies are limited to simple alkenes, alkynes, and imines as the unsaturated coupling partners. The use of alkyl formates as transfer hydroalkylating reagents with multiple unsaturated bond-containing substrates remains in its infancy, largely due to the issue of controlling their reactivity and selectivity (Scheme 1).

The reductive alkylation of *N*-heteroarenes offers an effective route to structurally diverse saturated N-heterocycles, which are valuable scaffolds in the design of pharmaceuticals, bioactive molecules, agrochemicals, functional materials, ligands, sensors, pigments, and dyes.[6] However, achieving direct and selective functionalization of *N*-heteroarenes remains challenging due to their high thermodynamic stability, their kinetic inertness, and the tendency of the heteroatom's lone pair to deactivate metal catalysts.[7] Only a few strategies are available to realize the synthesis under metal catalysis.[8] Furthermore, *N*-heteroarenes are challenging substrates compared with simple imines and alkenes in terms of selectivity and mechanism. Herein, we report a reductive hydroalkylation cascade of pyridine-fused *N*-heteroarenes that possess multiple reducible sites (*e.g.* imine and alkene units) by utilizing a well-defined (*N*–*N*–*N*)Cr(III) pincer complex as a catalyst[9] and alkyl formates as transfer hydroalkylating reagents. The use of chromium salts has emerged as an alternative to precious metal catalysts because of their low cost, acceptably low toxicity, and abundance in nature.[10] Nevertheless, this is the first example of Cr catalysts for dearomative reductive transformations of pyridine, quinoline, and other *N*-heteroarenes.

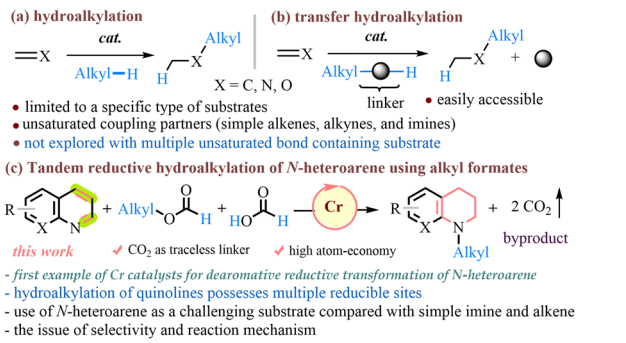

Scheme 1 Hydroalkylation and transfer hydroalkylation of unsaturated bonds.

Department of Chemistry, Indian Institute of Technology Guwahati, Guwahati-781039, Assam, India. E-mail: adas@iitg.ac.in

Table 1 Optimization studies[ab]

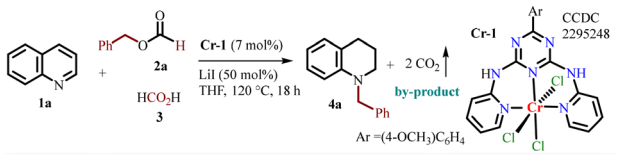

Entry	Deviation from the conditions above	Yield of **4a** (%)
1	With 30 mol% LiI	47%
2	None	83% (15%, **1a**)
3	KI, ZnI_2, Bu_4NI instead of LiI	0%, 0%, 0%
4	LiCl, $LiClO_4$ instead of LiI	0%
5	NaI (0.5 equiv.)	31%
6	$LiClO_4$ (0.2 equiv.) + NaI (0.5 equiv.)	46%
7	With 3 mol% of **Cr-1**	31%
8	With $CrCl_3{\cdot}3THF$, $CrCl_2$ instead of **Cr-1**	62%,[c] 15%
9	At 100 °C instead of 120 °C	23%
10	For 8 h	41%
11	DMF, DMSO, CH_3CN, toluene	23%, 56%, 0%, 0%
12	Without formic acid **3**	17% (72%, **1a**)

[a] Reaction conditions: **1a** (0.5 mmol), **2a** (0.5 mmol), formic acid **3** (1 mmol), **Cr-1** (7 mol%), LiI (0.25 mmol), stirred in THF (1.5 mL) at 120 °C for 18 h in a sealed tube. [b] Isolated yield. [c] Along with byproduct, *N*-formyl THQ, was isolated in 12% yield.

Our investigation commenced with the reaction of quinoline (**1a**, 1 equiv.), benzyl formate (**2a**, 1 equiv.), and formic acid (**3**, 2 equiv.) in the presence of the (*N*–*N*–*N*)Cr(III) complex **Cr-1**[9] (7 mol%) in THF at 120 °C (Table 1, S3 and S4). After 18 h, no desired product **4a** was obtained under the reaction conditions. Gratifyingly, in the presence of LiI (30 mol%), *N*-benzyl tetrahydroquinoline **4a** was obtained in 47% yield (entry 1). With a further increase of the LiI loading to 50 mol%, we were pleased to observe an 83% yield (entry 2). Alternative metal halides (*e.g.* potassium and zinc) showed negligible reactivity (entries 3 and 4). Combining NaI with a Lewis acidic metal successfully facilitated the reaction, underscoring the crucial role of both the iodide and Lewis acid (entries 5 and 6). The yield of **4a** was decreased by reducing the catalyst loading to 3 mol% (entry 7) or by using the simple chromium salt instead of *N*-ligated Cr complex Cr-1 (7 mol%) (entry 8). The yield of **4a** was also decreased by reducing the reaction temperature (entry 9) or by shortening the reaction time (entry 10). Screening other solvents revealed that highly polar solvents such as DMF and DMSO resulted in significantly reduced yields (entry 11). In the absence of formic acid **3**, product **4a** was obtained in only 17% yield, suggesting the importance of **3** in the reaction (entry 12).[11]

With the optimized reaction conditions in hand, we probed the scope of various functionalized quinolines **1a–1aw** using formate **2a** as the standard alkylating agent (Table 2). The substrates having both electron-donating and electron-withdrawing groups at different positions in the aryl moiety were efficiently reacted to obtain the desired products **4a–4w** in 27–85% yields. Notably, the retention of reducible functional groups (6-Cl, 6-Br, 6-OCOPh, 5-NO_2, 5-C≡CPh, 7-Cl, 7-Br, 7-NO_2, 7-OBn, and –CO_2Me) in the final products highlighted the excellent chemoselectivity of the present reductive protocol. The structures of the compounds **4l** and **4w** were unambiguously

Table 2 Substrate scope[ab]

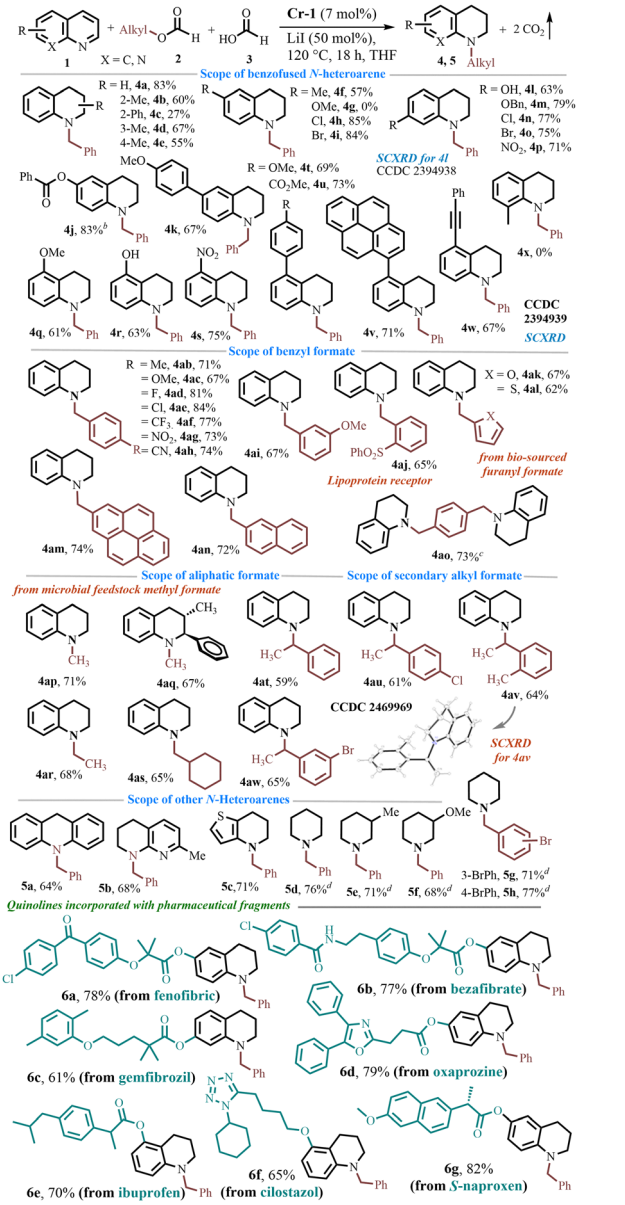

[a] Reaction conditions: **1a** (0.5 mmol), **2a** (0.5 mmol), formic acid **3** (1 mmol), **Cr-1** (7 mol%), LiI (0.25 mmol), stirred in THF (1.5 mL) at 120 °C for 18 h in a sealed tube, isolated yield. [b] With 0.5 mmol LiI. [c] With 0.25 mmol formate. [d] With 1 mmol LiI.

confirmed by single-crystal X-ray diffraction analyses (SC-XRD). Slightly higher yields were realized for electron-withdrawing groups. Free hydroxyl functionalities afforded desired *N*-alkylated products **4l** and **4r**, demonstrating the effectiveness of the base-free reaction conditions. The reactions with pyrene-tethered quinoline proceeded smoothly to provide the product **4v** in 71% yield. Next, benzyl formates **2a–2j**, with electron-poor and electron-rich groups, were subjected to the reaction conditions with **1a** and gave *N*-benzyl THQs **4ab–4aj** in 65–85% yield. The formates containing nitro (**2g**), nitrile (**2h**), and sulfonyl (**2j**) functionalities provided the products **4ag–4aj** efficiently. The

methodology was successfully utilized to synthesize a lipoprotein receptor **4aj**. The biosourced furfuryl formate **2k**, thiophen-2-ylmethyl formate **2l**, polyaromatic containing formates **2m–2n** and 1,4-phenylenebis(methylene) diformate **2o** were also smoothly transformed (**4am–4ao**), underscoring the broad applicability of this approach to diverse heterocyclic structures.

The use of methyl formate **2p** as a microbial feedstock can also lead to the biologically relevant *N*-methyl tetrahydroquinoline derivatives **4ap** and **4aq**. It is worth mentioning that compound **4aq** was observed exclusively in the trans-diastereomer under the reaction conditions. In the case of secondary benzylic formates **2s–2v**, although the cleavage of the C–O bond is more difficult than that of the primary benzylic formate, desired alkylated products **4at-4aw** were obtained in moderate to good yields. Additionally, the structure of **4av** was confirmed by SC-XRD. Interestingly, other related pyridine-fused *N*-heterocycles **1y–1ad** were successfully converted into the targeted *N*-alkylated compounds **5a–5d** under the optimized conditions. Unfortunately, isoquinoline, pyrimidine and indole were incompatible with this process. In general, pyridines are more challenging to reductively alkylate due to their high energy barrier to dearomatization, lower reactivity and strong tendency to coordinate with the active site. The current method was extended to a pyridine-based substrate, affording **5d–5h** in good yields.

Considering that the functionalization of *N*-benzyl THQs into biomedical molecules could result in renewed physicochemical properties and improve the metabolic stability,[6] we conducted late-stage transformation of several quinolines decorated with pharmaceutical fragments under standard conditions. The functionalized quinolines (**1ae–1ak** from fenofibric, bezafibrate, gemfibrozil, oxaprozin, ibuprofen, and naproxen) underwent smooth reductive dearomatization and *N*-alkylation cascade, affording the desired products **6a–6g** in good yields. These findings highlight the wide functional group tolerance and the promising potential of the current chemistry in further drug development.

Next, the method was used to the concise synthesis of cilostazol, a marketed pain-relief drug **7** *via* late-stage α-methylene C–H oxidation of **6f**,[12] further demonstrating the practical utility of this protocol (Scheme S23). Furthermore, the practicality of the reaction was extended to *C*-functionalized THQ derivative 9 in one pot by using *para*-quinone methide 8 as an alkylating precursor (Scheme S24). Then, following this developed protocol, natural alkaloid cuspareine **10** was directly synthesized from styryl quinoline **1al** and microbial feedstock **2p** (Scheme S25). Moreover, the reaction was viable even with consecutive double bond bearing quinoline **1am**, yielding the product **11** in 72% yield (Scheme S26). Notably, compounds **5d**, **5g** and **5h** were found as the key intermediates for the synthesis of paroxetine **12**, HDAC inhibitor **13** and histamine H3 receptor **14**, respectively (see SI, Scheme S22).[13] To showcase the practical applicability of this protocol, a gram-scale synthesis of **4a** was successfully conducted (Scheme S29). Then, the methodology's sustainability was evaluated using green chemistry metrics,[14] yielding an atom economy of 62.6%, an atom mass efficiency of 50%, a carbon efficiency of 76.2%, and a reaction mass efficiency of 49.7%, demonstrating environmental advantages (see SI, Section 9). There were no by-products; only volatile CO_2 was formed, which can be separated easily. Furthermore, the evolved CO_2 was trapped efficiently as a bench-stable amine carbamate ammonium salt **15** (Scheme S28), and this can be utilized as a reagent and catalyst for different organic transformations.

To obtain insight into the reaction pathway, a series of control experiments was performed (see SI, Section 5). First, to determine the possible intermediate in the reaction, the reaction was examined with quinolinium salt **I1** and *N*-benzyl-1,2-dihydroquinoline **I2** independently, in the presence of **2a** and **3** under standard conditions (Schemes S4 and S5). The desired product **4a** was obtained in quantitative yields, suggesting that the reaction likely proceeded through quinolinium salt **I1**, and the 1,2-dihydroquinoline **I2** intermediate. Conversely, the yield of **4a** with THQ **I3** is quite low (34%), and therefore, **I3** may not be an intermediate in the catalytic cycle (Scheme S6). When formate **2a** was reacted with 1 equivalent of LiI under the reaction conditions, benzyl iodide was obtained in 71% yield, showing that LiI promotes the cleavage of the C–O σ-bond to form the iodinated electrophile and lithium formate (Scheme S7). The presence of 12-crown-4 led to a decrease in the yield of **4a** (21%) and using NaI (instead of LiI) provided the product **4a** in 31% yield, indicating that the lithium ion played an important role in the given transformation (Schemes S8 and S9). Furthermore, control experiments using LiOCHO instead of LiI provided no desired product **4a**, pointing to the crucial role of iodide in the reaction. To validate the homogeneous catalytic system for the alkylation reaction, the mercury drop test was conducted, showing no inhibition of the reaction or reduction of the product yield (Scheme S3). To probe the mechanism of the reaction, the regio-specificity of hydrogen transfer with the deuterated benzyl formate (**2a-D**) and deuterated formic acid-d_2 (**DCO_2D**) was investigated for **1a** (Scheme 2). The use of **2a-D** resulted in the formation of **4a-d_1** with 92% deuterium incorporation at the C4-position. This suggests that formate hydrogen is successfully transferred to the *N*-heteroarene. A second experiment with deuterated formic acid-d_2 led to the formation of **4a-d_4** with deuterium incorporated into the C2-and C3-positions. Deuterium-labeling experiments with **1a-*d*** (>88% D) indicate no H/D scrambling product at the C4-position, suggesting that an intramolecular 1,3-H shift might not occur under the current reaction conditions (Scheme S16). In summary, the deuterium-labeling experiment

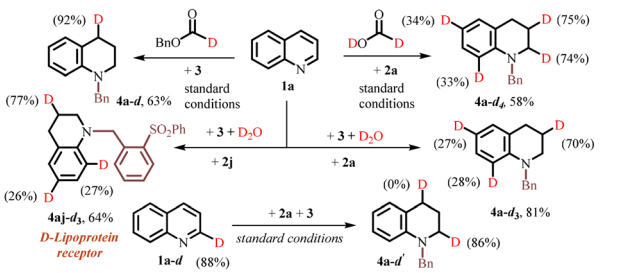

Scheme 2 Reaction pathway and deuteration of N-heteroarenes.

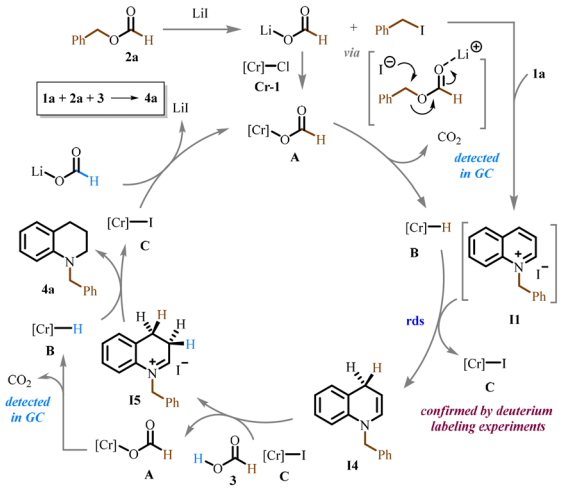

Scheme 3 Proposed pathway for the formation of the *N*-alkylated product.

suggests that the reaction pathway involves a stepwise 1,4-addition, followed by a 2,3-addition. Furthermore, in the presence of D_2O, 70% deuterium incorporation at the C3-position was observed. In addition, deuterium incorporation was detected at the C6- and C8-positions, which is likely the result of hydrogen isotope exchange (HIE) processes facilitated by the HCO_2D present in the reaction mixture.[15] We also synthesized the deuterated lipoprotein receptor **4aj-*d*$_3$** with adequate deuterium incorporation at the C3-position, highlighting the practical utility of the given method.[16] In the presence of radical scavengers such as 1,1-diphenylethene (DPE), butylated hydroxytoluene (BHT), and 9,10-dihydroanthracene (DHA), the reaction is not affected, suggesting that the radical-based MHAT pathway[17] is not likely to be involved in the given transformation (Scheme S17). To investigate the rate-determining step of the reaction in detail, a series of kinetic experiments was conducted. The results suggested first-order rate dependence on quinoline **1a** and the catalyst, and zero-order dependence on formate **2a** and LiI (Fig. S3–S6, SI). These data suggested that substrate **1a** and the catalyst are kinetically relevant; formate **2a** and LiI might not be involved in the rate-determining step. Furthermore, the electronic effect of the quinoline substrate on the rate of the reaction was examined (Schemes S18–S21). A competitive reaction suggested that an electron-withdrawing group (–Cl) on the quinoline enhanced the rate of the reaction with respect to an electron-donating group (–Me). In contrast, there is little electronic effect of the formate. Based on the electronic effect and order dependence, one can postulate that the addition of metal hydride to the activated quinolinium salt is likely to be the rate-determining step.[18] On the basis of previous reports[4f,19] and the present experimental findings, a plausible catalytic cycle has been proposed as shown in Scheme 3. First, formate **2a** is activated by the LiI to generate a reactive electrophile alkyl iodide ($PhCH_2I$) and a formate salt [Li][HCO_2]. The Lewis acidity of lithium(I) may help to cleave the C–O bond in the formate. The intermediate [Li][HCO_2] can react with **Cr-1** to form formate species **A**. The resulting chromium formate A undergoes decarboxylation under the reaction conditions to provide chromium hydride species B and releases CO_2. The presence of CO_2 was confirmed by the GC analysis of the gas phase. Meanwhile, *in situ* generated alkyl iodide can react with **1a** to produce quinolinium salt **I1**. The resulting metal hydride **B** is a potent reductant, able to reduce the activated quinolinium salt **I1** by forming the *N*-alkyl-1,4-dihydroquinoline **I4** intermediate. The resulting enamine **I4** isomerizes to an iminium species **I5** and is then reduced *via* a 1,2-hydride addition, affording the product **4a**.

In summary, the reductive alkylation of *N*-heteroarenes to saturated azacycles using alkyl formates as bifunctional reagents has been accomplished using a chromium catalyst. Its versatility enables late-stage diversification of complex structures and deuteration of quinolines. Notably, this environmentally benign strategy offers several advantages, including high conversion efficiency and atom economy in the synthesis of valuable N-heterocyclic products, while utilizing readily available starting materials, such as *N*-heteroarenes and alkyl formates, without requiring flammable hydrogen gas.[8]

A. D. gratefully acknowledges the ANRF, DST (CRG/2022/01606) for financial support. DST-FIST(SR/FST/CS-II/2017/23c), the CIF, IITG and NECBH (BT/CoE/34/SP28408/2018 and BT/NER/143/SP44675/2023) are acknowledged for NMR and X-ray facilities. A. P. would like to thank MoE for his PMR Fellowship. A. B. thanks the IITG for his research fellowship. We are grateful to the reviewers for their critical inputs to improve the manuscript.

Conflicts of interest

There are no conflicts to declare.

Data availability

The data supporting this article have been included as part of the supplementary information (SI). Supplementary information: experimental details, crystallographic data, compound data for characterization, and NMR spectra of new compounds. See DOI: https://doi.org/10.1039/d5cc06076a.

CCDC 2394938 (**4l**), 2394939 (**4w**) and 2469969 (**4av**) contain the supplementary crystallographic data for this paper.[20a–c]

References

1 S. W. M. Crossley, C. Obradors, R. M. Martinez and R. A. Shenvi, *Chem. Rev.*, 2016, **116**, 8912.
2 (*a*) S. Bonciolini, T. Noël and L. Capaldo, *Eur. J. Org. Chem.*, 2022, e202200417; (*b*) J. Peng, R. Bai and Y. Lan, *Acc. Chem. Res.*, 2025, **58**, 1484; (*c*) F. Mo and G. Dong, *Science*, 2014, **345**, 68.
3 (*a*) T. Sawano, K. Ogihara, J. Sagawa, M. Ono and R. Takeuchi, *Org. Lett.*, 2020, **22**, 6187; (*b*) P. M. Edwards and L. L. Schafer, *Chem. Commun.*, 2018, **54**, 12543.
4 (*a*) Y. Takada, S. Hayashi, K. Hirano, H. Yorimitsu and K. Oshima, *Org. Lett.*, 2006, **8**, 2515; (*b*) G. Li, R. Chen, L. Wu, Q. Fu, X. Zhang and Z. Tang, *Angew. Chem., Int. Ed.*, 2013, **52**, 8432; (*c*) T. Uchikura, K. Moriyama, M. Toda, T. Mouri, I. Ibáñez and T. Akiyama, *Chem. Commun.*, 2019, **55**, 11171; N. Chen, X.-J. Dai, H. Wang and C.-J. Li, *Angew. Chem., Int. Ed.*, 2017, **56**, 6260; (*d*) L. Yu, L. Lv, Z. Qiu, Z. Chen, Z. Tan, Y.-F. Liang and C.-J. Li, *Angew. Chem., Int. Ed.*, 2020, **59**, 14009; (*e*) L. Yin, M. Kanai and M. Shibasaki, *J. Am. Chem. Soc.*,

2009, **131**, 9610; (*f*) E. Crochet, L. Anthore-Dalion and T. Cantat, *Angew. Chem., Int. Ed.*, 2023, **62**, e202214069.
5 H.-M. Huang, P. Bellotti, J. Ma, T. Dalton and F. Glorius, *Nat. Chem. Rev.*, 2021, **5**, 301.
6 I. Muthukrishnan, V. Sridharan and J. C. Menéndez, *Chem. Rev.*, 2019, **119**, 5057.
7 H. Jia, Z. Tan and M. Zhang, *Acc. Chem. Res.*, 2024, **57**, 795.
8 M. G. Manas, J. Graeupner, L. J. Allen, G. E. Dobereiner, K. C. Rippy, N. Hazari and R. H. Crabtree, *Organometallics*, 2013, **32**, 4501.
9 P. Adhikari, N. Hazarika, K. Bhattacharyya and A. Das, *Org. Lett.*, 2024, **26**, 286.
10 (*a*) A. K. Steib, O. M. Kuzmina, S. Fernandez, D. Flubacher and P. Knochel, *J. Am. Chem. Soc.*, 2013, **135**, 15346; (*b*) X. Cong and X. Zeng, *Acc. Chem. Res.*, 2021, **54**, 2014; (*c*) F. Kallmeier, R. Fertig, T. Irrgang and R. Kempe, *Angew. Chem., Int. Ed.*, 2020, **59**, 11789.
11 The possible involvement of hydrogen iodide in the catalytic process is mentioned in the SI, Section 5.4.
12 M. Konwar, T. Das and A. Das, *Org. Lett.*, 2024, **26**, 1184.
13 (*a*) D. Chamorro-Arenas, A. A. Nolasco-Hernández, L. Fuentes, L. Quintero and F. Sartillo-Piscil, *Chem. – Eur. J.*, 2020, **26**, 4671; (*b*) Y. Takahashi, Y. Ashikari, M. Takumi and A. Nagaki, *Eur. J. Org. Chem.*, 2020, 618; (*c*) R. Apodaca, C. A. Dvorak, W. Xiao, A. J. Barbier, J. D. Boggs, S. J. Wilson, T. W. Lovenberg and N. I. Carruthers, *J. Med. Chem.*, 2003, **46**, 3938.
14 R. A. Sheldon, *Chem. Commun.*, 2008, 3352.
15 (*a*) T. Bhatt, T. Dutta, K. Yaswanth, V. N. Kalevaru, S. Wohlrab and K. Natte, *Chem. Commun.*, 2025, **61**, 12305; (*b*) E. Appert, A. Martin-Mingot, O. Karam, F. Zunino, B. Michelet, F. Bouazza and S. Thibaudeau, *Chem. – Eur. J.*, 2022, **28**, e202201583.
16 D. Ambrosek, M. Danz, H. Fluegge, J. Friedrichs, T. Grab, A. Jacob, S. Seifermann, D. Volz and M. Mydlak, *PCT Int. Appl.*, WO 2016116510A1, 2016.
17 J. Zhong, X. Wang, M. Luo and X. Zeng, *Org. Lett.*, 2024, **26**, 3124.
18 M. Pang, *et al.*, *Nat. Commun.*, 2020, **11**, 1249.
19 (*a*) J. Wu, W. Tang, A. Pettman and J. Xiao, *Adv. Synth. Catal.*, 2013, **355**, 35; (*b*) J. Wu, C. Wang, W. Tang, A. Pettman and J. Xiao, *Chem. – Eur. J.*, 2012, **18**, 9525.
20 (*a*) CCDC 2394938: Experimental Crystal Structure Determination, 2025, DOI: 10.5517/ccdc.csd.cc2ld427; (*b*) CCDC 2394939: Experimental Crystal Structure Determination, 2025, DOI: 10.5517/ccdc.csd.cc2ld438; (*c*) CCDC 2469969: Experimental Crystal Structure Determination, 2025, DOI: 10.5517/ccdc.csd.cc2nx6f7.

